

See discussions, stats, and author profiles for this publication at: <https://www.researchgate.net/publication/231275526>

Caging of Molecules by Asphaltenes. A Model for Free Radical Preservation in Crude Oils

ARTICLE *in* ENERGY & FUELS · APRIL 2000

Impact Factor: 2.79 · DOI: 10.1021/ef990206p

CITATIONS

31

READS

49

4 AUTHORS, INCLUDING:



Vladimiro Mujica

Arizona State University

140 PUBLICATIONS 3,111 CITATIONS

SEE PROFILE



Luis Puerta

Universidad de Carabobo, UC

8 PUBLICATIONS 36 CITATIONS

SEE PROFILE



Socrates Acevedo

Central University of Venezuela

111 PUBLICATIONS 1,265 CITATIONS

SEE PROFILE

Caging of Molecules by Asphaltenes. A Model for Free Radical Preservation in Crude Oils

Vladimiro Mujica,^{*,†} Pedro Nieto,[†] Luis Puerta,[†] and Socrates Acevedo^{*,‡}

Laboratorios de Físico Química y Físico Química de Hidrocarburos, Universidad Central de Venezuela, Facultad de Ciencias, Escuela de Química, 47102, Caracas, 1041 Venezuela

Received September 24, 1999. Revised Manuscript Received January 26, 2000

Using a hybrid computational strategy, based on semiempirical quantum chemical (ZINDO) and molecular mechanics estimations of interaction energies, as well as experimental data in the literature, a caging model for free radicals in crude oil is proposed. In this model, the free radical is efficiently shielded by asphaltenes, protecting these reactive species from hydrogen transfer and other reactions and preserving them through geological times in the crude. The relevance of this model to important properties of asphaltenes, such as solubility and aggregation, is discussed. The complex asphaltenes were modeled as polycyclic aromatic hydrocarbons (PAH). Our calculations showed that the intermolecular interaction energy for the R...T vdW complex, consisting of molecular fragments R and T, was more negative when one subsystem (R or T) was a free radical, suggesting that these radicals could easily be involved in aggregation. Support for these ideas was also found in the relatively large stabilization energy calculated for a paramagnetic vanadyl–porphyrin–pyrene complex, consistent with the known behavior of metallic petroporphyrins found in asphaltenes. Possible implications and generalization of this model for related chemical systems are also analyzed.

Introduction

The problem of molecular aggregation is pervasive and of considerable importance in several branches of science, ranging from polymers to colloids and emulsions. The optical, magnetic, and electric properties of these systems are strongly influenced by aggregation. One of the most striking consequences of the formation of molecular aggregates is the stabilization of reactive species, notably free radicals, in chemically aggressive environments. In this article, we use both computational and experimental results to propose a model for a particular instance of aggregation of asphaltenes, where the phenomenon itself is driven by the higher stability of free radical aggregates. The model might have important implications for related systems.

Asphaltenes are very important components of petroleum. They are precipitated from crude oils by the addition of large quantities (40 v or more) of a low molecular weight paraffin (usually, pentane or heptane¹). This amorphous solid is a complex mixture of compounds, and in relation to other crude oil components, asphaltenes have lower hydrogen-to-carbon ratio (H/C), generally between 0.9 and 1.2; higher aromaticity (f_a), around 40%; higher heteroatom content (such as sulfur, nitrogen, oxygen, vanadium, nickel); higher average molecular weight (M);² higher free radical or

spin concentration (S_0);^{3–6} and higher concentration of metal–porphyrines.⁷ Spectroscopic as well as chemical studies have shown that the main components of asphaltene structure are polycyclic aromatic systems, substituted with aliphatic, alicyclic, and heteroatoms groups.

Asphaltenes are important in the oil industry, due to their deleterious effects in many industrial operations (production, refining, and transportation). Many of these problems are related to the capacity of the sample to form aggregates and flocs in the crude, leading to formation damages, clogging of rock pores and production facilities, catalysis fouling, and deposit formation during storage, among other inconveniences.

Therefore, many research efforts have been dedicated to the study of the relevant factors in asphaltene aggregation. It is known that asphaltenes are in the form of small colloidal particles (around 5 nm diameter) in the crude oil and in nonpolar organic solvents, such as benzene and toluene;⁸ that these aggregates are dissociated by polar solvents such as pyridine, THF, and

* Corresponding authors. E-mail (Acevedo): soacevedo@strix.ciencs.ucv.ve.

[†] Laboratorio de Físico Química.

[‡] Laboratorio de Química de Hidrocarburos.

(1) Method IP 143. 1990, 9–12.

(2) *Chemistry of Asphaltenes*; Bunger, J. W., Li, N., Eds.; Am. Chem. Soc. Symp. Ser. 1981, 195. This book presents a comprehensive review of the subject.

(3) Yen, T. F.; Erdman, J. G.; Saraceno, A. J. *Anal. Chem.* 1962, 34, 694–700.

(4) Nnuzuma, S.; Steele, C. T.; Gunnings, H. E.; Strausz, O. P. *Fuel* 1977, 56, 249–256.

(5) Schultz, K. F.; Selucky, M. L. *Fuel* 1981, 60, 951–956.

(6) Galtsev, V. E.; Ametov, I. M.; Grinberg, O. Y. *Fuel* 1995, 74, 670–673.

(7) (a) Yen, T. F. *The Role of Trace Methods in Petroleum*; Yen, T. F., Ed.; Ann Arbor Science: Ann Arbor, MI, 1975; Chapter 1, pp 1–30. (b) Branthaver, J. F.; Dorence, S. M. *ACS, Div. Pet. Chem.* 1977, 22, 727–728. (c) Espinoza Pena, M.; Marijarrez, A.; Campero, A. *Fuel Process. Technol.* 1996, 46, 171–182. (d) Ysambertt, F.; Márquez, N.; Rangel, B.; Bauza, R. *Sep. Sci. Technol.* 1995, 30, 2539–2550.

(8) Sheu, E. Y.; Storm, D. A. *Asphaltenes: Fundamentals and Applications*; Sheu, E. Y., Mullins, O. C., Eds.; Plenum Press: New York, 1995; Chapter 1, pp 1–52.

nitrobenzene; and that they aggregate in dilute solutions of nonpolar solvents,² probably below 100 mg L⁻¹.⁹

In a previous communication, a solvent fractionation of a Venezuelan sample of Cerro Negro asphaltene was presented.¹⁰ The solid-liquid Soxhlet extraction was performed from 40% to 100% THF, using an acetone-THF gradient. Seven solid fractions (*f_i*) were obtained in this way. It was found that the solubility *S_i* of the fraction obtained decreased when both *f_a*(*i*) and *S_d*(*i*) increased. It was reported, that *f₇* (12% of the sample), corresponding to 100% THF was insoluble in all common organic solvents (toluene, THF, pyridine, chloroform, etc.) and 85% of the asphaltene fraction has a poor solubility in toluene (<1 mg L⁻¹).

The presence of free radicals in asphaltenes, detected long ago,³ is a very intriguing fact. This is because these radicals are among the most reactive species in organic chemistry, and to our knowledge a radical such as the one expected in this case (polycyclic aromatic), has never been isolated in pure form. As suggested in the above referred work,¹⁰ survival of free radicals would be possible by the shielding provided by other aromatic compounds in the aggregate. In this way, the free radical will remain "caged" and preserved against chemical reactions.

Striking evidence of this chemical protection for the radical species is provided by the EPR measurements of spin concentration which remains sizable despite the use of strong free radical eliminators.¹⁰ In fact, the most relevant reaction in this case would be hydrogen transfer, which suggests that the caging should be very effective and that reactive hydrogens could neither enter nor be present in the cage. In any case, this "caging effect" would be a particular example of the general aggregation phenomenon in asphaltenes. As discussed below, this could have very important consequences in the solubility and aggregation behavior of the sample.

In this paper we present a theoretical study of this problem. For this purpose we used a hybrid methodology which employs both molecular mechanics (MM+), and quantum mechanical tools. The approach, widely used in the literature to model complex systems,¹¹⁻¹³ consists of an energy minimization using MM+ to determine plausible geometries of the molecular complex, followed by a more detailed quantum chemical study of the electronic energy surface. Since detailed structural information about asphaltenes is yet lacking, we have considered PAH that can be thought of as reasonable chemical precursors and/or fragments of the larger and more complex asphaltenes. Using the theoretical results obtained, and the above-mentioned solubility and *S_d* data, we propose a plausible model for the caging effect

and analyze its consequences in connection with the behavior of metal-porphyrines complexes. As shown below, both theoretical and experimental results support the existence of the caging phenomenon.

Methods

For simplicity we will use the symbol R...T for the complex between molecules R and T. Following the suggestion¹⁴ we refer to these complexes as van der Waals (vdW) molecules. Also, closed shell aromatic systems (even number of carbons) and aromatic radicals (open shell, odd number of carbons) will be referred as even (E) or odd (O) systems, respectively. Complexes between them will be denoted EE and OE vdW molecules. Since radicals with an even number of carbons should be very reactive, perinaphthenyl (I), and other pericondensed radicals were selected as prototypes for odd molecules (see Figure 1). These are expected to be relatively stable.¹⁵

The ZINDO/1, ZINDO-CI, and molecular mechanics MM+ packages provided by Hyperchem were used. These ZINDO programs contain options for both Hartree-Fock and correlated calculations. The CI version was employed in all open shell calculations, using a range of 5 eV. For closed shells systems, no significant differences were found between the two ZINDO schemes, thus we used the ZINDO/1 in this case. In all calculations, initial equilibrium geometries were found using MM+.

The procedures described below were performed for the calculation of ΔE of formation of the vdW molecules for the reaction $R + T = R...T$.

1. MM+ Geometries and Energies (ΔE_{MM^+}) for R...T. Energies E^R , for R, E^T for T, and E^{RT} for R...T were optimized, and ΔE_{MM^+} was found as usual using eq 1:

$$\Delta E_{MM^+}^+ = E^{RT} - (E^T + E^R) \quad (1)$$

2. Calculations with a Constant Value for the σ and π Overlap Coefficients. In any semiempirical method there are adjustable parameters that are chosen to model selected properties of the system. Intermolecular energies of weakly bounded systems are very sensitive to parameters controlling the orbital overlap. In ZINDO these parameters are the coefficients $f_{\sigma\sigma}$ and $f_{\pi\pi}$.

In these calculations we used the values recommended in the Hyperchem package for these ZINDO coefficients; these are: $f_{\sigma\sigma} = 1.267$ and $f_{\pi\pi} = 0.64$. Initial geometries of R, T, and R...T were found using MM+. With this choice, the corresponding ZINDO energies E_z^R , E_z^T , and E_z^{RT} were computed and the corresponding energy difference, ΔE_z^{RT} was found by subtraction (see eq 1).

3. Calculations Where the σ Overlap Coefficient $f^{\sigma}(z)$ Is a Function of the Intermolecular Distance *z*. As reported in the literature, the use of ZINDO for the study of molecular interactions between PAH has a serious drawback in that a deep minimum appears

(9) Acevedo, S.; Ranaudo, M. A.; Pereira, J. C.; Castillo, J.; Fernández, A.; Pérez, P.; Caetano, M. *Fuel* **1999**, *78*, 997-1003.

(10) Acevedo, S.; Escobar, G.; Ranaudo, M. A.; Piñate, J.; Amorín, A. *Energy Fuels* **1997**, *11*, 774-778.

(11) Leach, A. R. *Molecular modeling, principles and Applications*; Addison-Wesley Longman Ltd.: 1996; p 524.

(12) (a) Treboux, G. *J. Phys. Chem.* **1994**, *98*, 1054-1062. (b) Treboux, G.; Maynau, D.; Malrieu, J. P. *J. Phys. Chem.* **1995**, *99*, 6417-6423.

(13) (a) Field, M. J.; Bas, P. A.; Karplus, M. J. *J. Comput. Chem.* **1990**, *11*, 700-733. (b) Field, M. J.; Bash, P. A.; Karplus, M. J. *J. Am. Chem. Soc.* **1987**, *109*, 8092-8094. (c) Chandrasekhar, J.; Smith, S. F.; Jorgensen, W. L. *J. Am. Chem. Soc.* **1984**, *106*, 3049-3050. (d) Brown, F. K.; Singh, U. C.; Kollman, P. A.; Raimondi, L.; Kouk, K. N.; Bock, C. W. *J. Org. Chem.* **1992**, *57*, 4862-4869.

(14) Hobza, P.; Zahradnik, R. *Intermolecular Complexes, The role of van der Waals System in Physical Chemistry and the Biodisciplines*; Academia: Praga, 1988; Chapter 1, p 25.

(15) Acevedo, S.; Ranaudo, M. A.; Gutiérrez, L.; Escobar, G. *Fuel* **1996**, *75*, 1139-1144.

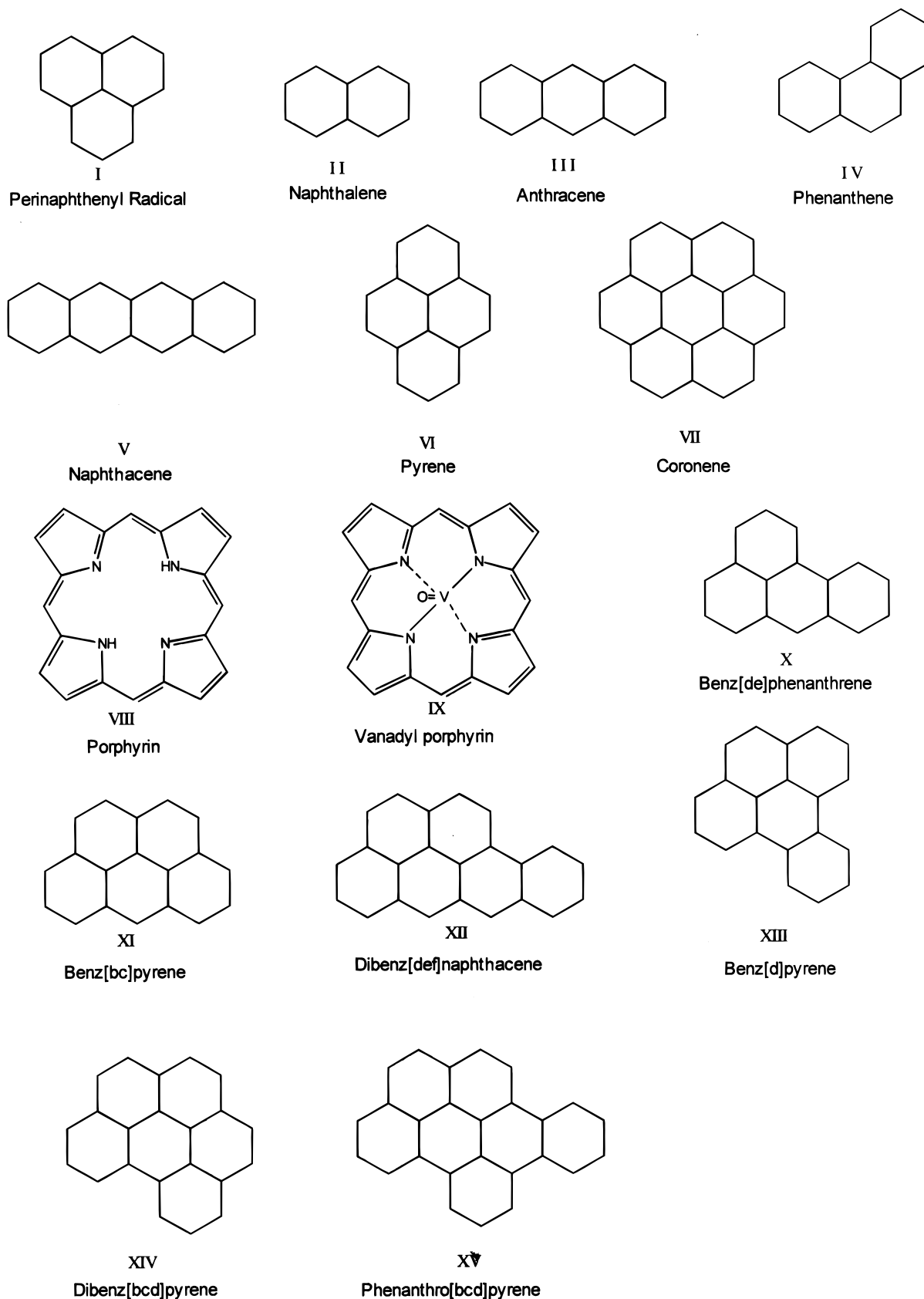


Figure 1. Structures of model compounds used in this work. Compounds I, X, XI, and XII are odd (radicals) polycyclic aromatics.

corresponding to a spurious chemical bond at around 2.5 Å.¹⁶ To correct for this fact, we used a modification of the method proposed by Sadygov and Lim,¹⁶ which is based on the eqs 2 and 3, for the correction of the σ overlap factor of the ZINDO program:

$$f^*(z) = f[1 - \exp(7.49 - 4.05z)] \quad \text{for } z \leq 3.5 \text{ Å} \quad (2)$$

$$f^*(z) = f[1 - \exp[-(4.90 + 0.51z)]] \quad \text{for } z \geq 3.5 \text{ Å} \quad (3)$$

where $f^*(z)$ should be between 0 and 2.

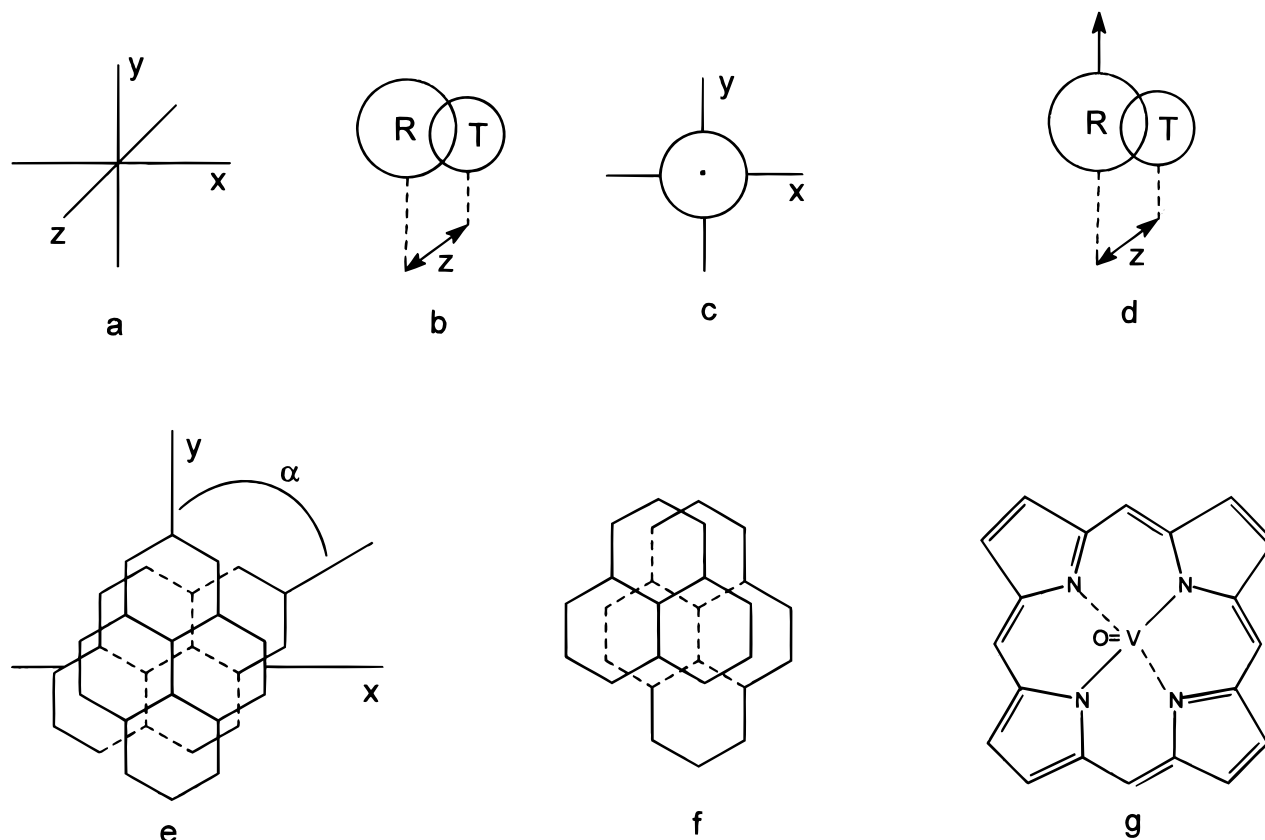


Figure 2. Geometrical models used in this work. (a) Coordinate system. (b) and (c) In eclipsed conformations of $R \cdots T$, R is placed on top of T with both centers of mass at the points, R: $(0,0,z)$, T $(0,0,0)$. Then R could be moved along y (d) or x . (e) Illustration of dihedral angle α . (f) Eclipsed conformation for the perinaphthyl-pyrene complex. (g) Model for vanadyl porphyrin. When required, the center of mass of pyrene $(0,0,z)$ was placed on top of the vanadium atom $(0,0,0)$ in eclipsed conformation.

To use this method we proceed as follows: An initial value is given to the constant f . Then the corresponding E^T , E^R , and E^{RT} are computed at each selected value of the intermolecular distance z using the $\bar{F}(z)$ found by means of eqs 2 and 3. In this way, optimum values for E^{RT} (minimum), for the intermolecular distance (z_1) and for ΔE^{RT} were found. This procedure is repeated as many times as required with a new f value in each cycle. In this way, sets of ΔE^{RT} and z_1 values are obtained for each f . Then, to select the best f value, plots of ΔE^{RT} against f , and of ΔE^{RT} vs z_1 were made (see below).

In these calculations, geometries of R and T were obtained from MM^+ at each selected z value and kept during the ZINDO calculation.

4. Exploration of Electronic Potential Energy Surface. In the required cases, we explored the ground-state electronic potential energy surface of the vdW molecule in the neighborhood of the MM^+ geometry assumed for the calculation of ΔE^{RT} . For this, we proceeded as follows: a MM^+ (procedure 1 above) or ZINDO (procedure 2) minimum was found by keeping molecules R and T in an eclipsed conformation as depicted in Figure 2. This allowed the determination of the intermolecular distance (z_1) for this conformation. Starting from this point, and fixing T in the xy plane, R was moved along the x axis, along the y axis, or rotated about the z coordinate (the dihedral α angle, see Figure 2). ZINDO calculations were then performed for all these points and computed values of ΔE^{RT} plotted against the relevant coordinate.

5. Porphyrin Calculations. Since MM^+ does not have parameters for vanadium, we use the following geometry pseudooptimization: According to the literature the vanadium atom should be placed in the plane of the porphyrin ring between the nitrogen atoms.¹⁷ To obtain this, it was required to begin the MM^+ calculations with the vanadium bonded to the four nitrogen atoms. Once the optimization was obtained, the two extra bonds were deleted. ZINDO calculations of the corresponding $R \cdots T$ vdW molecules were performed as above, using eclipsed conformations (see Figure 2).

Results

In Table 1 ΔE^{RT} and z_1 values, calculated using procedures 1 and 2 above are shown. When the values of ΔE_{MM}^{RT} were plotted against the number of carbons in the complex, n_C , the following line was obtained:

$$\Delta E_{MM}^{RT} = -0.755 + 0.3739 n_C \quad r^2 = 0.991 \quad (4)$$

Here, n_C is the total number of carbons in the $R \cdots T$ molecule and the energy is in kcal/mol. In this plot we include the EE and OE complexes considered in Table 2. This clearly shows that MM^+ cannot differentiate between these vdW molecules. According to eq 4, the slope indicates that about 370 cal/mol should be added to the interaction for each carbon atom in the complex.

(16) Sadygov, G.; Lim, C. *Chem. Phys. Lett.* **1994**, 225, 441–447.

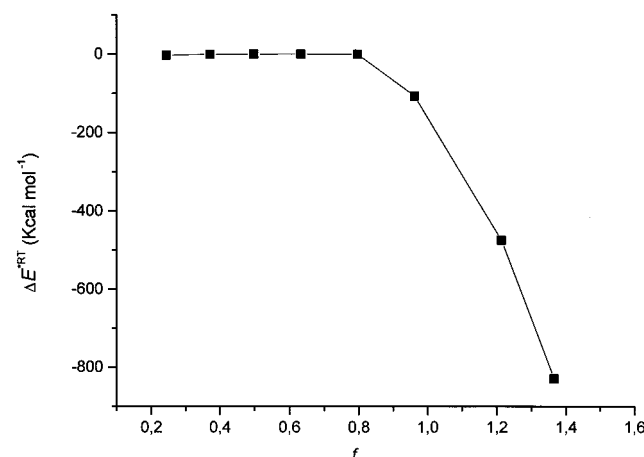
(17) Plato, M.; Tränkle, E. J.; Lubitz, W.; Lendzjan, F.; Möbns, K. *Chem. Phys.* **1986**, 107, 185–196.

Table 1. ΔE^{RT} and Intermolecular Distance z_1 Calculated by ZINDO and MM⁺ for Several vdW Complexes^a

complex ^b	n_C ^c	$-\Delta E^{\text{RT}}$ (kcal mol ⁻¹)		z_1 (Å)
		MM ⁺	ZINDO ^d	
1 I–II	23	7.87	87	3.41
2 I–III	27	9.40	105	3.42
3 I–IV	27	9.56	104.7	3.55
4 I–V	31	10.30	86.8	3.50
5 I–VI	29	10.29	27.8	3.43
6 I–VII	37	12.80	177.8	3.37
7 II–VI	26	8.80	1.14	3.41
8 II–II	32	11.45	1.5	3.43
9 II–VII	40	14.46	2.4	3.36

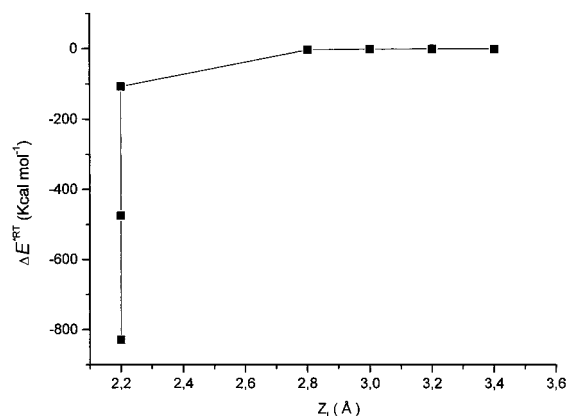
^a Geometry of complexes obtained from MM⁺ in all calculations.^b See Figure 1. ^c Number of carbon atoms in complex. ^d ZINDO-CI for open shell (rows 1–6) and ZINDO-I for closed shell (rows 7–9) calculations.**Table 2.** Computed Minimum Energy Change (ΔE^{RT})^a and Intermolecular Distances (z_1) for the Pyrene–Pyrene (EE) and Perinaphthyl–Pyrene (OE) Complexes for Assumed Values of f ^{a,b}

f	$-\Delta E^{\text{RT}}$ (kcal mol ⁻¹)		z_1 (Å)	
	EE	OE	EE	OE
0.25	3.27	3.84	2.8	2.6
0.375	0.65	1.73	3.0	2.6
0.5	0.18	1.10	3.2	2.8

^a Using procedure 3. These values were calculated in the low energy regions (see Figures 3–6). ^b Overlapping coefficient was changed with z (see text).**Figure 3.** Plot of ΔE^{RT} minimum vs f for the pyrene dimer using procedure 3.

In Figures 3 and 4 the plots of ΔE^{RT} vs f and of ΔE^{RT} vs z_1 for the pyrene dimer (EE complex) are shown. These optimum values were computed as described in procedure 3 above (see the Methods section). Similar plots were obtained for the complex pyrene–perinaphthyl (OE complex). From these plots is evident that beyond some limiting f (close to 0.8 in the EE case and to 0.5 in the OE case) a very fast drop in ΔE^{RT} is observed when f is increased. However, below these limits reasonably steady values of ΔE^{RT} were obtained. Hence, values of the parameter f in this stable region can safely be used, thereby eliminating the spurious chemical minimum found for short distances.

In Table 2 values of ΔE^{RT} and z_1 for values of f corresponding to the upper flat portions of the ΔE^{RT} plots (see Figures 3 and 4) are shown. It is clear from Table 2 that for any assumed f , the energy change for

**Figure 4.** Plot of minimum ΔE^{RT} vs f intermolecular distance for the pyrene dimer using procedure 3. With $f = 0.375$.

the OE system is more negative. Accordingly, the corresponding z_1 equilibrium distances are smaller.

In Figure 5 profiles of ΔE^{RT} against the intermolecular distance z for the pyrene dimer and for the pyrene–perinaphthyl are shown. These were calculated assuming $f = 0.375$ and the eclipsed conformations shown in Figure 2g. Corresponding ΔE^{RT} and z_1 for the minima could be found in Table 2.

Using the geometry corresponding to z_1 in Table 2 and the eclipsed conformation as reference, an exploration of the potential energy surface around the minimum was performed (see above). Good behavior was found in all cases. A sample of results is shown in Figure 6, parts a–c for the EO complex. As shown in these figures, reasonably wide intervals were examined for the x , y , and α coordinates. These results suggest that, within the approximated ZINDO scheme employed, the behavior of ΔE^{RT} around z_1 is the expected for the principal minimum.

In Table 3, ΔE^{RT} and n_C values for several complexes are shown. Eclipsed conformations were used for these calculations. After a search for the best f , the values in Table 3 were computed using $f = 0.265$.

When the energy values of Table 3 were plotted against n_C , the following linear regressions were found:

$$\text{EE: } \Delta E_z^{\text{RT}} = -2.313 - 0.102 n_C \quad r^2 = 0.985 \quad (5)$$

$$\text{OE: } \Delta E_z^{\text{RT}} = -1.8875 - 0.148 n_C \quad r^2 = 0.997 \quad (6)$$

Figure 7 shows the potential energy profiles for the porphyrin complexes studied (see the Methods section for other details). These were computed using the eclipsed conformation described in Figure 2 and $f = 0.265$ (see Table 3).

Discussion

Reliability of ZINDO Calculations. According to the results in Table 1, use of the ZINDO methods, combined with MM⁺, leads to an overestimation of the association energy ΔE_z^{RT} for the perinaphthyl complexes (OE). Besides, no clear trend is found when the different ZINDO energies are compared. No improvement of these results was found when we use the UHF version of ZINDO. Also, no significant changes were observed when the points near the MM⁺ minimum were examined (see procedure 2 above).

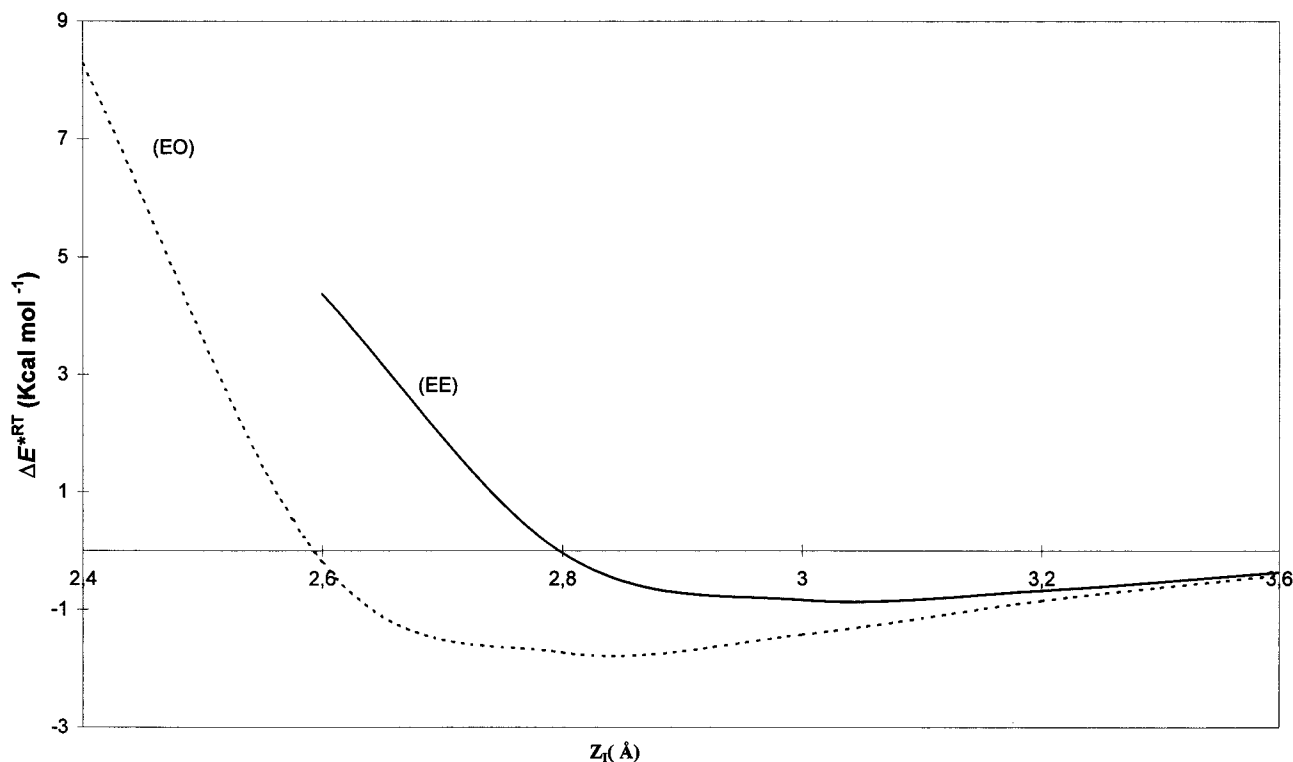


Figure 5. Profiles of ΔE^{*RT} vs z_1 for pyrene-pyrene (EE) and pyrene-perinaphthyl (EO) complexes with $f = 0.375$.

Table 3. ΔE^{RT} Values for Several Complexes Calculated Using the ZINDO Methods Described in Procedure 3^a

complex type ^b				$-\Delta E^{RT}$ (kcal mol ⁻¹)	
OE ^b	n_C ^c	EE ^b	n_C ^c	OE	EE
I-VI	29	(VI) ₂	32	6.17	5.61
X-XIII	37	(XIII) ₂	40	7.34	6.54
XI-XIV	41	(XIV) ₂	44	8.06	6.61
XII-XV	49	(XV) ₂	52	9.11	7.73

^a $f = 0.265$ was used. ^b See Figure 1 for identification of compounds. ^c Number of carbon atoms in the complex.

However, better results were found when the σ overlapping factor was allowed to change with distance (f^* , see eqs 2 and 3, Tables 2 and 3, and Figure 7). Figures 3 and 4 show very clearly that unless f^* is chosen in the right interval, f^* will be too large and bonding factors will be overestimated leading to unrealistic bonding energies.

Of course, no unique f value could be expected from this treatment. This in fact was the case for the pyrene dimer and for the pyrene-perinaphthyl complex, which required different f 's in two different calculations (see Figure 7 and Table 3). However, in this work we are interested in differences in the energy of formation between EE and EO complexes. As shown in Table 2, this difference is reasonably independent of f .

According to the ZINDO calculations (see Table 3) the EO complexes are more stable than the EE ones (see below). Comparison of the slopes of eqs 5 and 6 suggest that the stabilization energy for the OE falls 1.45 times faster for the OE case.

When the energy per carbon atom of the different methods are compared, some interesting implications emerge (see eqs 4-6). To a good approximation, both ZINDO and MM⁺ ΔE^{RT} values are linearly dependent on n_C .

For MM⁺ this is the expected result for aromatic hydrocarbons since the empirical potential is a summation over bonds terms.¹⁸ Of course MM⁺ cannot distinguish between EE and OE complexes because no parameters for free radicals are included in this program. Besides, such difference is entirely of quantum origin, being the result of dispersion interaction (see Appendix) and therefore cannot be accounted for by any classical potential.

Moreover, the results shown in Table 3 suggest that for EE and OE vdW molecules, the association energy increases steadily with the molecular weight, M , an expected result for vdW complexes.

In view of these favorable features, and for the purpose of the present work, we believe that with the proper choice of parameters, the above ZINDO calculations are reliable.

Relevance of Calculations to Experiments. In this work we used PAH as prototypes for the simulation of the relevant intermolecular associations in asphaltenes. There are several reasons for this, such as the high f_a of this sample, the increase of S_d with f_a , the expected dependence of the caging effect on polarizability, etc. Besides, reactive hydrogens, such as the one in aliphatic and heteroatoms groups are not expected in the neighborhood of a reactive radical. These arguments suggest that PAH should be good models, simple enough to allow electronic structure calculations to be carried out. Inclusion of aliphatic and heteroatoms groups in a systematic way requires a more extensive parametrization which is now underway.

1. Free Radicals. Now using these calculations as background, we will discuss the data mentioned above,¹⁰ related to caging of radicals and solubility (see the Introduction), a new result and other reports in the

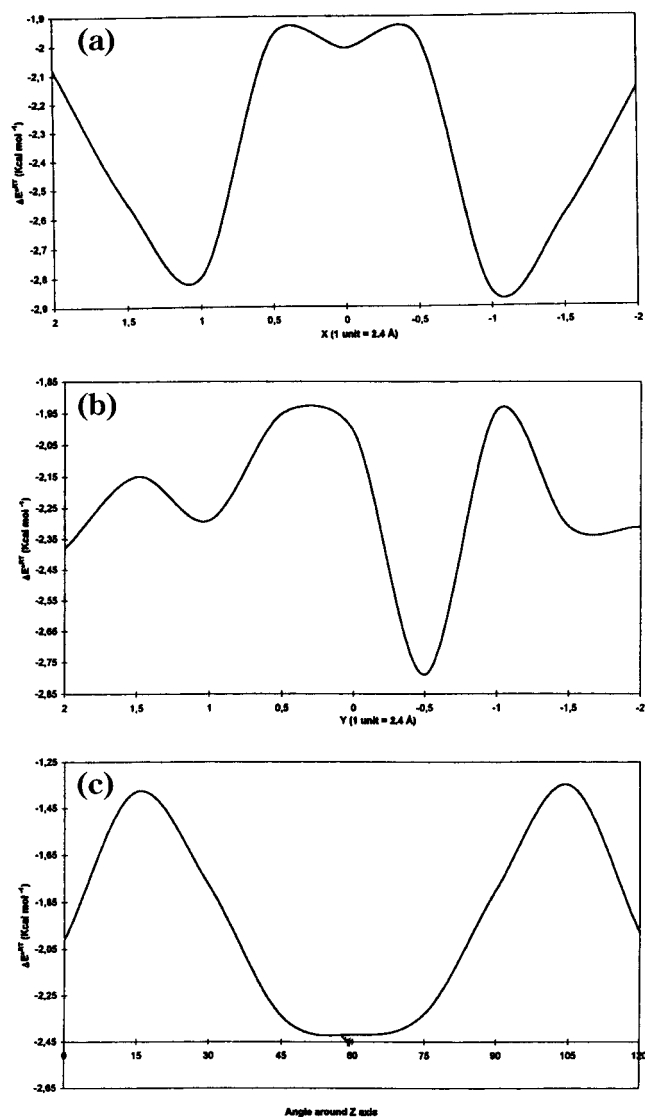


Figure 6. Profiles of ΔE^{RT*} around the minimum for the pyrene-perinaphthyl (EO) complex. (a) Along x axis, (b) along y axis, (c) angle around z axis.

literature. From our calculations it is clear that, in general, a free radical or lone electron will promote aggregation to a larger extent than the corresponding closed shell systems. Since aggregation is a common place in asphaltenes, it should be expected that all radicals in crude oil will be trapped or caged by this sample. Or, more precisely, by their aromatic sections since these are the more abundant and polarizable sections of them. This caging or encapsulation is enhanced by the lone electron, and the radical will be isolated from the media leading to a reduced reactivity. As reported earlier,¹⁰ this would justify its presence in crude oils.

It is well-known that asphaltene aggregates can be dissociated in polar solvents.^{2,8} For instance, M measurements in polar solvents (pyridine, THF) render lower values than in nonpolar solvents (toluene, benzene). It was reported in the work under discussion, that when the asphaltenes were boiled in THF, the initial S_d value was reduced to 1/3 S_d .¹⁰ From the above discussion a reduction is expected since dissociation will expose some radicals to solvent attack. Those which

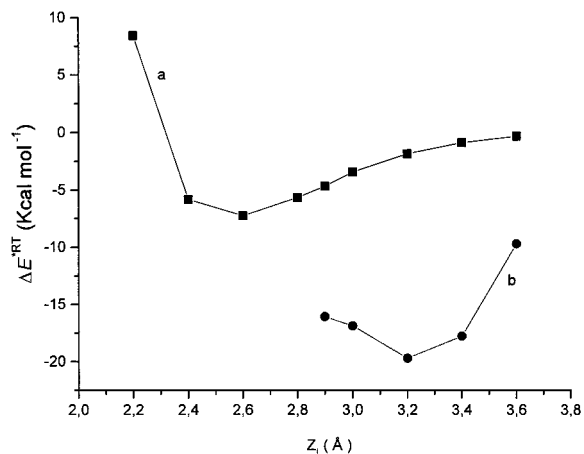


Figure 7. Comparison of energy profiles for the porphyrin-pyrene (a) and vanadylporphyrin (b) complexes using $f = 0.375$.

survive are probably very well encapsulated or trapped in a high molecular weight environment (see Table 3).

Due to their easy detection by EPR, and to the chemical reactivity factors discussed above, radicals are very convenient markers for the caging effect. However, since the above trapping of radicals should be a particular case of aggregation, encapsulation of molecules by asphaltenes should be a general effect under favorable conditions. For instance, the reduction in solubility is likely to be a consequence of this effect. As some relatively loosely trapped compounds are removed from the solid by the extraction solvent, the remaining solid would form stronger bonds leading to a solubility drop. This would justify the high solubility of the entire sample (asphaltenes) and the low solubility of the fractions f_i .

Using the procedure described,¹⁰ we measured a $S_d = 1.6 \times 10^{19}$ spin g⁻¹ for Furrial asphaltenes. This value is higher than the values reported in the literature for eight asphaltenes from different locations around the world which average around $(2.2 \pm 0.9) \times 10^{18}$,³ and also higher than one reported¹⁰ for Cerro Negro asphaltenes (9.2×10^{18}). Furrial is a Venezuelan crude oil with serious asphaltene precipitation problems,¹⁹ whereas, to our knowledge, none of the other asphaltenes present this difficulty. Although more data is required before reaching a final conclusion in this regard, these results and data suggest strongly that the S_d value could be a very valuable tool for predicting solubility behavior during production operations.

In a recent investigation, EPR was employed to propose short-range asphaltene aggregation and it was found that oxygen molecules bound to asphaltenes form stronger complexes than argon.²⁰ Since oxygen is paramagnetic, and argon is not, this result is expected.

2. Porphyrins. It is a fact known to any one working in the field, that the metal porphyrins naturally present in the crude oil, and called petroporphyrins, are very difficult to extract from the asphaltenes.^{7,21} This is always the case, regardless of the polarity of solvent used for the precipitation. Generally, strong polar

(19) Acevedo, S.; Ranaudo, M. A.; Escobar, G.; Gutiérrez, L.; Ortega, P. *Fuel* **1995**, 74, 595–598.

(20) Clericuzio, M.; Del Piero, G.; Scotti, R. *Appl. Magn. Reson.* **1998**, 14, 81–100.

(21) Baker, E. W. *Organic Geochemistry*; Eglinton, G., Murphy, M. T. J., Eds.; Longmans Ltd.: 1969; Chapter 19, p 468.

boiling solvents, such as acetone, methanol–pyridine mixtures, etc., are employed in the extraction, usually with poor results. Of course, the solubility of petroporphyrins in these solvents is very high, whereas the solubility of asphaltenes in them is very low.

From the above calculations and discussion, a comparatively strong association between the metal porphyrin and asphaltenes could be expected due to the presence of paramagnetic vanadium in this compound. This, and the above solubility properties of this substance are reasonably predicted by the above ZINDO calculations (see Figure 7). It is interesting that a relationship between aggregation kinetics and vanadium content has been reported for asphaltenes.²²

Conclusions

After a proper choice of the overlap parameter, reasonable results for vdW energies of formation for EE and OE aromatic complexes have been calculated using the ZINDO programs. These calculations show that paramagnetic or open shell complexes are more stable than the corresponding closed shell vdW molecules and support the idea that reactive free radicals should be present in crude oil encapsulated by asphaltene molecules. Other important properties of asphaltenes, such as solubility and aggregation, were appropriately discussed in terms of models and ideas derived from the calculations.

Acknowledgment. This work was supported by CONICIT Grants No. G97000722. We also thank Lic. Betilde Segovia for typing the manuscript.

Appendix

It is not difficult to see why one should expect that the OE interaction would be more stable than that corresponding to EE. Since we are dealing here with

low to nonpolar compounds, the main contributors to the stabilization energy of the vdW molecules would be the induction (E^I) and dispersion (E^D) energies. Both, E^I and E^D for the vdW molecule depend on the polarizability of the subsystems, i.e., on the ability of each subsystem to modify the electron configuration of the other. Since the bonding energy of the lone electron is very low, the OE complex would be more polarizable leading to a lower stabilization energy.

From a quantum mechanical perspective, E^I and E^D depend on the mixing of the ground-state wave function Ψ_0 with excited states Ψ_E of either subsystem. This mixing is due to the field imposed on one partner by the other. When such a field is treated as a perturbation, these energies could be obtained using perturbation theory. For instance, for E^I and E^D the following equations have been suggested:²³

$$E^I = \sum_{K=1}^{\infty} \frac{[\langle \Psi_K^R \Psi_0^T | P | \Psi_0^R \Psi_0^T \rangle]^2}{E_0^R - E_K^R} + \sum_{L=1}^{\infty} \frac{[\langle \Psi_0^R \Psi_L^T | P | \Psi_0^R \Psi_0^T \rangle]^2}{E_0^T - E_L^T} \quad (\text{A-1})$$

$$E^D = \sum_{K=1}^{\infty} \sum_{L=1}^{\infty} \frac{[\langle \Psi_K^R \Psi_L^T | P | \Psi_0^R \Psi_0^T \rangle]^2}{(E_0^R - E_K^R) + (E_0^T - E_L^T)} \quad (\text{A-2})$$

where $\Psi_0^{R(T)}$, $E_0^{R(T)}$, and $\Psi_{K(L)}^{R(T)}$, $E_{K(L)}^{R(T)}$ are ground-state and excited wave functions and energies corresponding to the subsystems R and T, and P is the perturbation operator. These terms are always negative (attractive) because the ground-state energies E_0^R and E_0^T are always smaller than the excited ones. When the subsystem R is a free radical, the energy denominators, E_0^R and $E_{K'}^R$, are small, compared to closed-shell systems, and therefore both E^I and E^D would be more negative.

Thus, both from intuition and from quantum mechanics an OE complex is expected to be more stable than a corresponding EE one.

EF990206P

(22) Yudin, I. K.; Nikolaenko, G. L.; Gorodetshii, E. E.; Markhashov, E. L.; Frot, D.; Briolant, Y.; Agayan, V. A.; Anisimov, M. A. *Pet. Sci. Technol.* **1988**, *16*, 395–414.

(23) See ref 14, Chapter 2, p 61.